PRAMANA — journal of physics

Vol. 80, No. 1
January 2013
pp. 89–103

Thermal-hydraulic analysis of LBE spallation target for accelerator-driven systems

ANISEH AHMED ATEF ABDALLA[1,*], JIYANG YU[1] and YONGWEI YANG[2]

[1]Department of Engineering Physics; [2]Institute of Nuclear and New Energy Technology, Tsinghua University, Beijing, 100084, China
*Corresponding author. E-mail: aniseh.abdalla@gmail.com

MS received 27 June 2011; revised 16 May 2012; accepted 12 July 2012

Abstract. In an accelerator-driven subcritical system (ADS), a high-performance spallation neutron source is used to feed the subcritical reactor. Neutron generation depends on the proton beam intensity. If the beam intensity is increased by a given factor, the number of generated neutrons will increase. The mechanism yielding a high rate of neutron production per energy is the spallation process, and this mechanism produces very high-energy deposition in the spallation target material. Producing a high rate of neutrons is accompanied by creation of problems of decay heat cooling and radiological protection. As a first step in designing a full-scale industrial ADS, a small-scale experimental ADS, which is similar to the European experimental ADS (XADS) is analysed. The analysis presented in this paper is based on lead–bismuth eutectic (LBE) cooled XADS-type experimental reactors, designed during the European experimental (PDS-XADS) project. Computational fluid dynamics analysis has been carried out for the spallation target. Steady-state behaviour and shear stress transport turbulence model with the automatic wall treatment were applied in the present analysis.

Keywords. Thermal-hydraulic analysis; accelerator-driven system; spallation target; shear stress transport; computational fluid dynamics.

PACS No. 28

1. Introduction

Today, the accumulation of huge quantities of long-lived radioactive waste is the biggest problem faced by the nuclear power industry. So, transmutation of long-lived radioactive nuclides using an accelerator-driven system (ADS) is considered to be a reasonable solution for reducing the long-term radiotoxicity of nuclear waste.

In order to design a full-scale industrial ADS, firstly, a small-scale experimental ADS which is similar to the European experimental ADS (XADS) is analysed. Computational fluid dynamics (CFD) [1] analysis has been carried out for the spallation target.

For ADS design, a subcritical reactor core with multiplication factor (Keff) in the range of 0.95–0.98 is a prerequisite. The subcritical reactor needs an external neutron source in order to maintain the reactor at the required level. Neutrons are produced by spallation process. When a high-energy proton beam inserted into the accelerator tube penetrates the window, the beam strikes a heavy element target, which produces a shower of neutrons. Producing a high rate of neutrons creates problems of decay heat cooling and radiological protection.

Three different types of ADS targets have been investigated by Sordo *et al* [2]. These are water-cooled solid target, gas-cooled solid target and window target which is lead–bismuth eutectic (LBE)-cooled. In this paper, the LBE-cooled target has been selected as the topic of study.

Lead–bismuth eutectic is a molten alloy with 44.8% lead (Pb) and 55.2% bismuth (Bi). One of the advantages of using LBE in ADS, is that Pb/Bi mixture can be used as coolant. LBE is used as spallation target as well as coolant. Thus, LBE allows good compatibility between the target and coolant. LBE's low melting temperature reduces the risk of uncontrollable freezing. The high boiling temperature of the LBE is an important safety feature to eliminate pressurization and boiling concerns while enhancing the inherent safety of the reactor core. LBE has excellent heat transfer properties and good chemical compatibility. These features make LBE an attractive spallation target.

The main objective of this paper is to analyse the thermal-hydraulic performance of the LBE flow. The temperature distribution analysis is carried out only in the window part, where the highest temperature distribution occurs. Sensitive analysis has been carried out for LBE flow parameters and window material parameters to show how these parameters affect the window's surface temperature.

2. Description of target geometry and material of construction

The design of the lower part of the PDS-XADS molten Pb–Bi target unit is depicted in figure 1. This figure shows the scheme of the target and the main geometrical data.

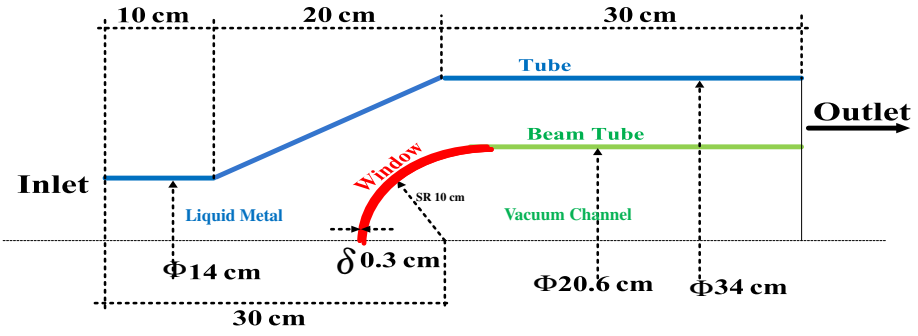

Figure 1. PDS-XADS spallation target.

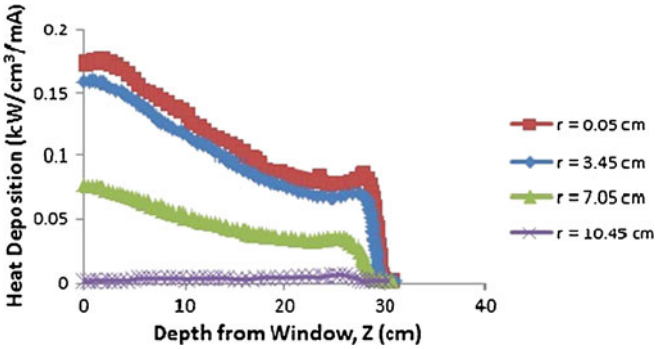

Figure 2. Heat deposition distribution in LBE flow, zero coordinate located at the centre of the window, which is at a distance of 30 cm from the inlet.

The thickness of the window of the spallation target is chosen as 3 mm, and the window material is the modified 9CrlMo ferritic-martensitic steel (T91). The reasons for choosing T91 as window material are its good mechanical strength and resistance to radiation. The thickness of the tube which contains the LBE and the thickness of the vacuum channel beam tube are ignored in our design.

The proton beam has a cylindrical shape with 8 cm radius and its intensity follows an elliptical radial distribution [3] as shown in eq. (1).

$$\Phi(r) = \frac{3I_0}{2\pi r_0^2}\sqrt{1-\left(\frac{r}{r_0}\right)^2}, \tag{1}$$

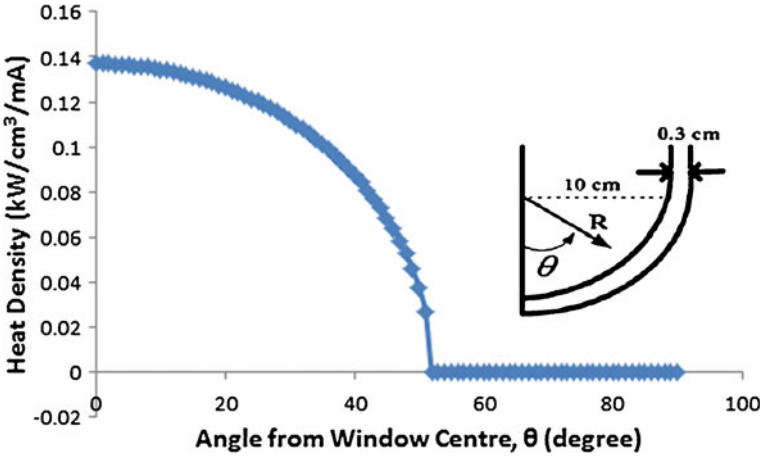

Figure 3. Heat deposition distribution on the window surface, zero coordinate located on the window pole which is at a distance of 19.7 cm from the inlet.

Table 1. Physical properties and parameters of LBE [4,5] (44.8 wt% Pb and 55.2 wt% Bi).

Property	LBE (T in °C)
Density (kg/m^3)	10737–1.375 T
Specific heat (J/kg K)	146.5
Dynamic viscosity (Pa s)	$3.26 \times 10^{-3} - 6.26 \times 10^{-6}$ T $+ 4.63 \times 10^{-9}$ T^2
Thermal conductivity (W/mK)	7.26 + 0.0123 T
Thermal expansibility (1/K)	$(7782.609-\text{T})^{-1}$
Melting temperature (K)	397.7
Boiling temperature (K)	1943

where I_0 is the total proton beam current, r_0 is the radius of the beam, and r is the radial distance from the axis of the beam. When 600 MeV proton beam with 6 mA proton current enters the vacuum beam tube, the proton beam penetrates the window and strikes the flowing LBE target. The spallation reaction caused by the bombardment of proton on the target leads to the generation of a shower of neutrons. Producing high rate of neutrons creates the problem of decay heat cooling. So, an efficient heat removal system is necessary to cool the high temperature of spallation and window materials.

Calculations of the heat deposition profile in the window and LBE have been carried out using MCNP-X code (which is a Monte Carlo radiation transport code). As observed in figures 2 and 3, the largest heat deposition density is in the LBE flow near the centre of the window [3]. Physical properties of the window material T91 and the fluid LBE material used in the CFD calculations are described in tables 1 and 2.

3. Numerical approach

Thermal-hydraulic analysis has been carried out by ANSYS CFX code. Steady-state behaviour and shear stress transport (SST) turbulence model with the automatic wall treatment were applied in the ANSYS CFX-Pre as boundary conditions.

Table 2. Physical properties and parameters of martensitic steel T91 [6–8].

Property	Window material T91
Density (kg/m^3)	7800
Specific heat (J/kg K)	562.69
Thermal conductivity (W/m°C)	-2×10^{-5} T^2 + 0.017T + 25.535
Melting point (°C)	1400
Young's modulus (GPa)	175
Dilatation coefficient (10^{-6}/K)	13

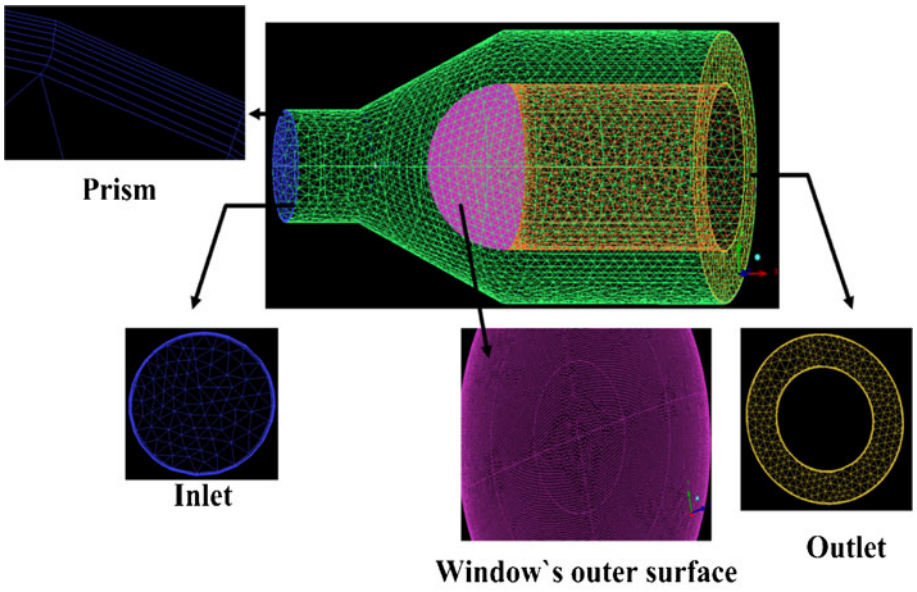

Figure 4. Unstructured mesh for the entire geometry.

Firstly, the geometry of the spallation target is created in ANSYS ICEM CFD, and then unstructured meshing has been created for the three-dimensional domain, and prism layers were applied around the walls (figure 4). Highest mesh density is applied to the region near the window, because the largest heat deposition is expected in that region. Secondly, after importing the mesh into the pre-processer, boundary conditions, fluid properties and window material properties are defined (table 3).

The simulation stopped after 120 iterations when the convergence criteria were met at 5.0×10^{-6}. This is called very tight convergence, which is sometimes required for geometrically sensitive problems.

Table 3. Boundary conditions applied by the system analysis.

Simulation type	Steady state
Turbulence	Shear stress transport
Wall function	Automatic
Inlet temperature (°C)	233
Inlet mass flow rate (kg/s)	198
Inlet turbulence	High (intensity = 10%)
Heat transfer on the tube wall	Adiabatic
Heat transfer on the beam tube wall	Adiabatic
Window heat deposition (kW)	39
LBE heat deposition (MW)	2.4

4. Results and analysis

The analysis is carried out for 600 MeV proton beam with 6 mA beam current; inlet mass flow rate is 198 kg/s and inlet flow temperature is 233°C. All the simulations have been carried out in a steady-state condition with turbulence flow regime. Turbulence flow regime is used to increase the coolant efficiency of LBE flow because most of the proton's energy is deposited as heat in the LBE target. Moreover, LBE is the spallation target as well as the coolant. LBE flow also cools down the window part.

4.1 *Velocity distribution of the spallation target*

As observed in figure 5, the highest flow velocity is in the inlet tube, where the red vectors appear. The maximum LBE flow velocity is 1.363 m/s. The highest flow velocity is less than the design velocity limit (2 m/s). Velocity flow is an important safety issue for avoiding erosion damage of the structural material. The stagnation flow is located in the pole of the window, where the blue vectors appear. This happened as we expected.

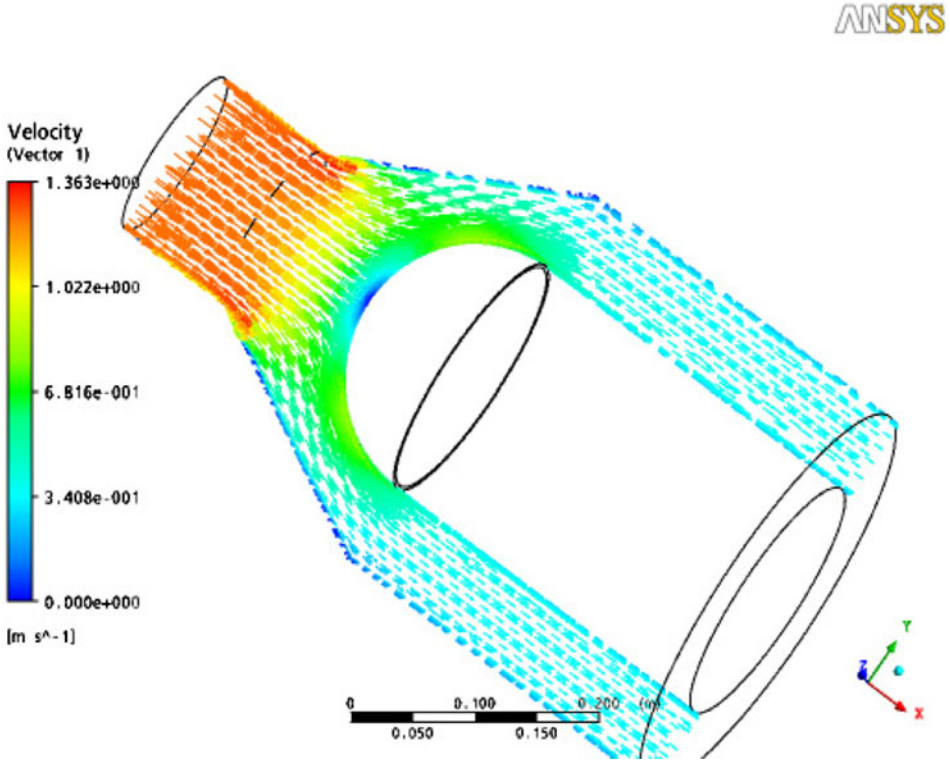

Figure 5. LBE flow velocity vector profile in the xy plane.

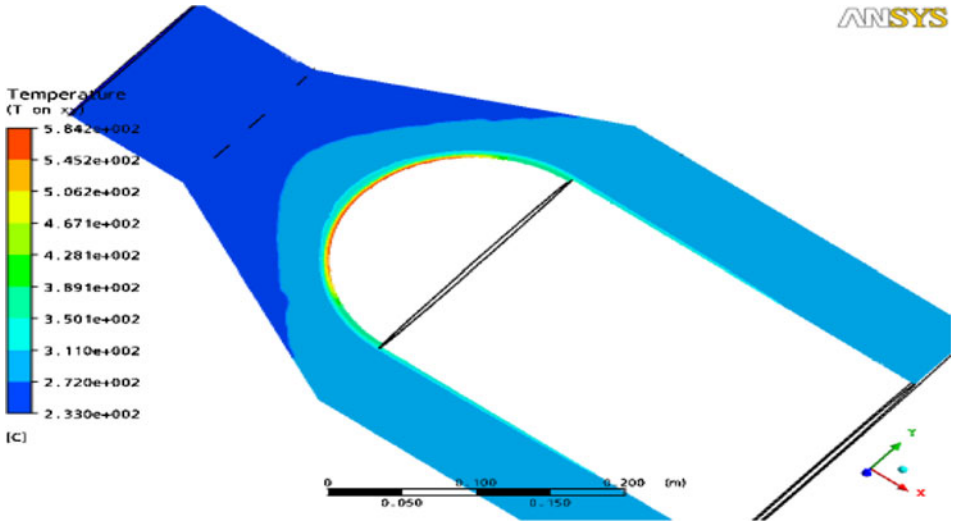

Figure 6. Temperature contour profile of LBE spallation targets in the xy plane.

4.2 *Temperature distribution of the spallation target*

The LBE flow inlet temperature is 233°C (figure 6). During the flow of LBE in the inlet tube, it removes the heat from the window and flows into the outer tube. Since the heat transfer is clearly seen between the window and the LBE flow, the temperature distribution along the LBE spallation target varies from 233°C to 584.36°C. The highest temperature

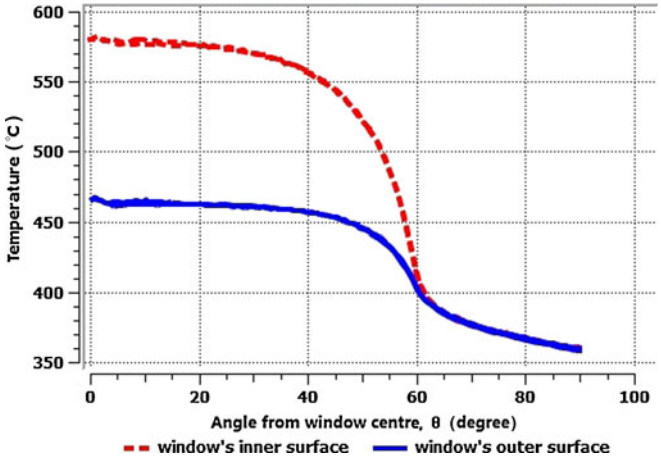

Figure 7. Window surface temperature distribution at high inlet turbulence (10% turbulence intensity).

Table 4. Results for spallation target at high inlet turbulence (10% turbulence intensity), with mass flow rate 198 kg/s and inlet temperature 233°C.

Parameters	High turbulence (intensity = 10%)
Average inlet temperature (°C)	233
Average outlet temperature (°C)	296.94
Temperature difference between windows surfaces, ΔT	113.2
Maximum LBE temperature (°C)	436.6
Maximum window temperature (°C)	584.36
Maximum window thermal stress (MPa)	128.77
Maximum LBE velocity (m/s)	1.363

is in the window pole where it reaches 584.36°C which exceeds the temperature design limit. This is where the stagnation point occurs. This is the reason why the window is not properly cooled. However, maximum temperature of the window must be lower than 525°C in order to avoid significant corrosion damage of the window.

Temperature differences between the outer and the inner surfaces of the window produce thermal stress. The thermal stress equation is

$$\sigma = \frac{\alpha \Delta T}{2} E. \tag{2}$$

α is the thermal linear expansion coefficient, ΔT is the temperature difference between the hotter and colder faces of the plate and E is the Young's modulus of the material. The thermal stress has to be much lower than its elastic limit (175 MPa) [8]. Otherwise, the window has to be replaced a few times a year to avoid corrosion damage. The maximum

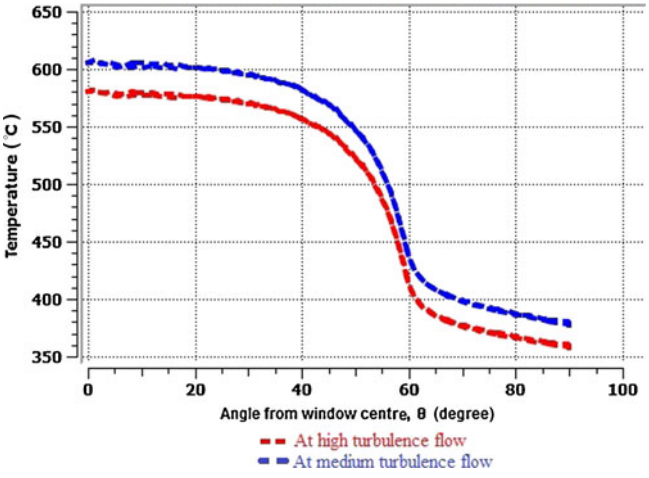

Figure 8. Window's inner surface temperature distribution at different inlet turbulences.

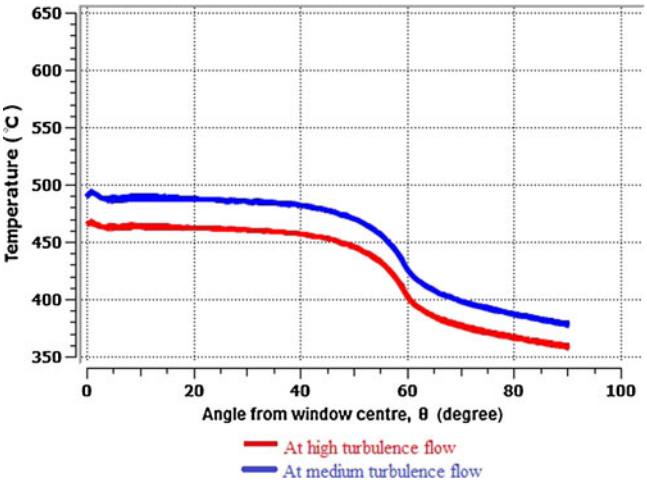

Figure 9. Window's outer surface temperature distribution at different inlet turbulences.

window thermal stress is 128.77 MPa, which is lower than the design limit (figure 7 and table 4).

4.3 *Effect of inlet turbulence*

In order to see how the turbulence intensities of LBE affects the window surface temperature, sensitivity analysis has been carried out for different turbulence intensities of LBE flow (figures 8 and 9).

Table 5 shows the simulation results with medium and high turbulence intensities of LBE inlet flow. As seen from the results mentioned above, the maximum window temperature distribution decreases by 28°C at high turbulence intensity of LBE in comparison to that at medium turbulence intensity. So, at high turbulence intensity, temperature distribution on the window decreases and better heat transfer can be achieved.

Table 5. Results for spallation target at different inlet turbulences with mass flow rate 198 kg/s and inlet temperature 233°C.

Parameters	Medium turbulence (intensity = 5%)	High turbulence (intensity = 10%)
Average inlet temperature (°C)	233	233
Temperature difference between window's surfaces, ΔT	112.6	113.2
Maximum LBE temperature (°C)	466.9	436.6
Maximum window temperature (°C)	612.8	584.36
Maximum window thermal stress (MPa)	128.1	128.77

Table 6. Results for spallation target at high inlet turbulence (high intensity = 10%), mass flow rate 198 kg/s and different inlet temperatures.

Parameters	$T_{\text{inlet}} = 134$ (°C)	$T_{\text{inlet}} = 167$ (°C)	$T_{\text{inlet}} = 200$ (°C)	$T_{\text{inlet}} = 233$ (°C)
Average inlet temperature (°C)	134	167	200	233
Temperature difference between window's surfaces, ΔT	113.2	113.2	113.2	113.2
Maximum LBE temperature (°C)	336.76	370	403.3	436.6
Maximum window temperature (°C)	488.2	520.2	552.2	584.36
Maximum LBE velocity (m/s)	1.34	1.35	1.356	1.363

4.4 *Effect of inlet temperature*

Sensitive analysis has been carried out for different inlet temperatures. These temperatures are 134°C, 167°C, 200°C and 233°C. Table 6 shows the details of the simulation results of the spallation target at different inlet temperatures.

As observed from the results above (figures 10 and 11), window surface temperature and LBE flow temperature increase by increasing inlet temperature, and LBE flow velocity increases by increasing inlet temperature. So, highest window surface temperature and highest LBE flow velocity occurred at an inlet temperature of 233°C. This is expected because in the steady-state flow system, the mass flow rate is constant. Mass flow rate

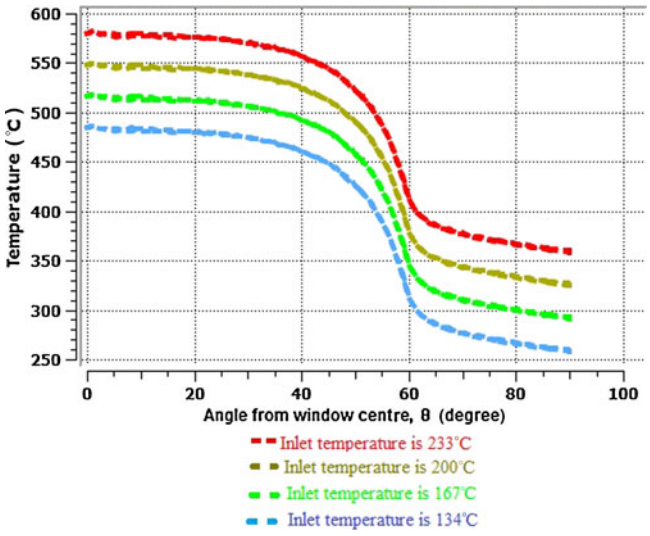

Figure 10. Window's inner surface temperature distribution at different inlet temperatures.

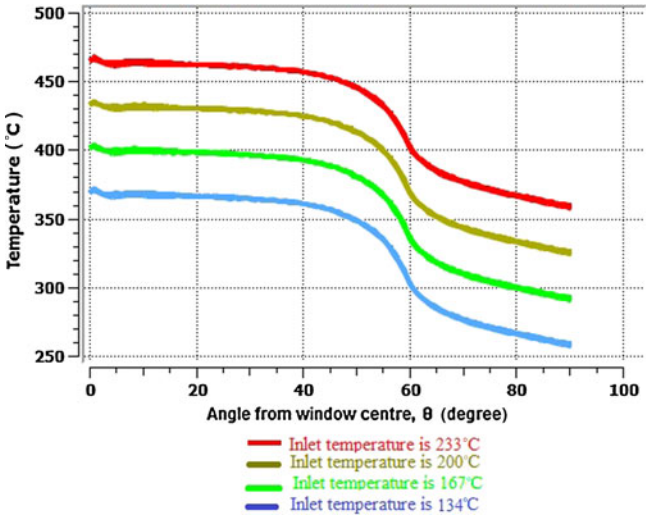

Figure 11. Window's outer surface temperature distribution at different inlet temperatures.

entering the spallation target tube has to be equal to the mass flow rate out of the spallation target tube.

$$\dot{m}_{\text{inlet}} = \dot{m}_{\text{outlet}}$$

(Continuity equation at steady state for single inlet and outlet)

$$m = \rho A V, \tag{3}$$

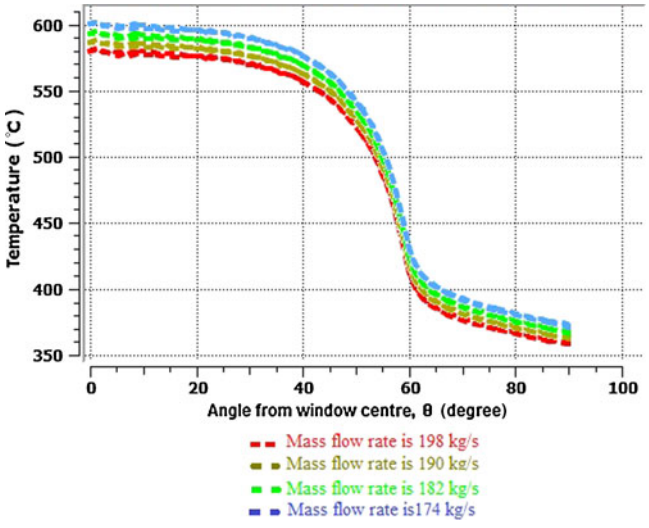

Figure 12. Window's inner surface temperature distribution at different mass flow rates.

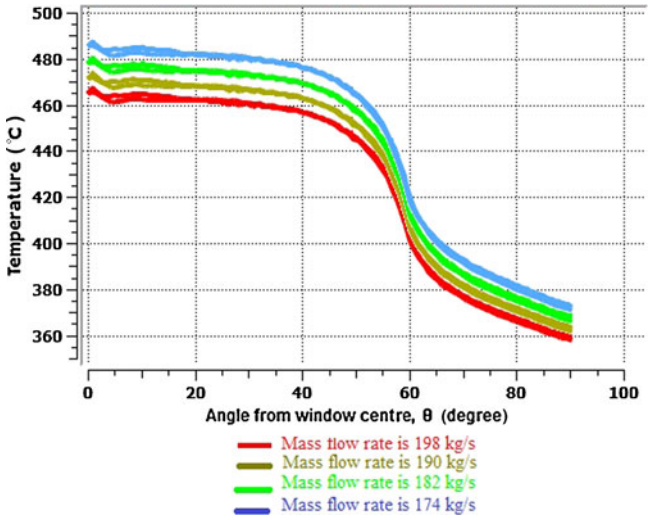

Figure 13. Window's outer surface temperature distribution at different mass flow rates.

where m is the mass flow rate, ρ is the flow density, A is the area of cross-section and V is the flow average velocity. When inlet temperature increases, LBE flow density decreases and consequently, flow velocity increases and mass flow rate remains constant.

4.5 *Effect of mass flow rate*

Sensitivity analysis has been carried out for different mass flow rates in order to see the effect of mass flow rate on window surface temperature and other parameters. These mass flow rates are 174, 182, 190 and 198 kg/s (figures 12 and 13).

According to the results in the tables 7, window surface temperature distribution decreases when inlet mass flow rate increases. All these results are obtained at the same

Table 7. Results for spallation target at high inlet turbulence (high intensity = 10%), inlet temperature 233°C and different inlet mass flow rates.

Parameters	Mass flow rate = 174 kg/s	Mass flow rate = 182 kg/s	Mass flow rate = 190 kg/s	Mass flow rate = 198 kg/s
Average inlet temperature (°C)	233	233	233	233
Temperature difference between window's surfaces, ΔT	113.1	113.2	113.2	113.2
Maximum LBE temperature (°C)	457.6	450.1	443.1	436.6
Maximum window temperature (°C)	604.6	597.3	590.6	584.36
Maximum LBE velocity (m/s)	1.196	1.25	1.31	1.363

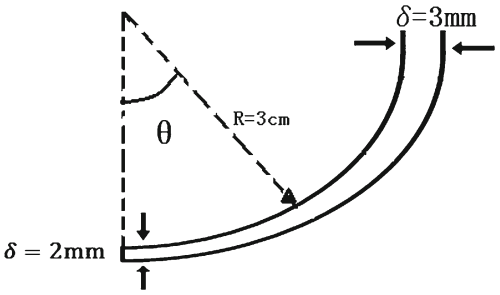

Figure 14. Schematic view of the window thickness with the improved design.

inlet temperature of 233°C and with different mass flow rates of LBE flow. According to the continuity equation at steady state flow system, when the mass flow rate increases, the flow velocity also increases. When the mass flow rate is as high as 198 kg/s, LBE velocity is also high. Subsequently, the window surface is better cooled.

4.6 *Effect of the window thickness*

When protons with high energy hit the spallation target, a number of neutrons are produced by spallation reactions with large amount of heat deposition in the LBE target and in window. LBE flow properly cools the target. But, the window pole is not properly cooled because of the stagnation point. So, it would be very difficult to keep the window temperature below the design limit (525°C), which is an important design limit challenge. In order to improve the initial design of the spallation target material, the window

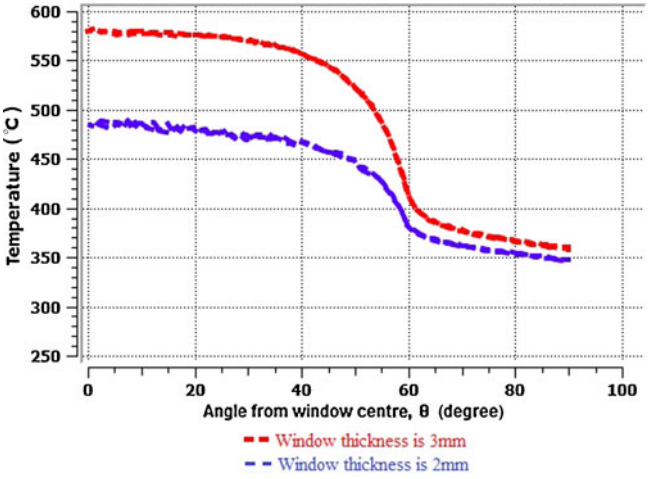

Figure 15. Window's inner surface temperature distribution for the initial design (3 mm window thickness) and improved design (2 mm window thickness).

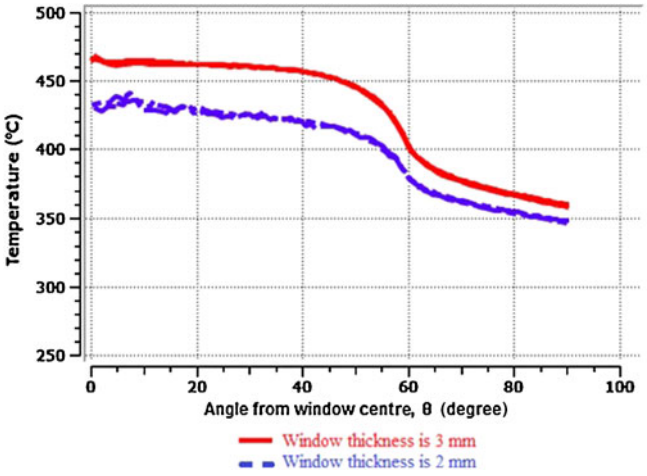

Figure 16. Window's outer surface temperature distribution for the initial design (3 mm window thickness) and improved design (2 mm window thickness).

Table 8. Results for spallation target at different window thicknesses with high inlet turbulence (high intensity = 10%), inlet temperature 233°C and inlet mass flow rate 198 kg/s.

Parameters	Improved design (window thickness is 2 mm)	Initial design (window thickness is 3 mm)
Average inlet temperature (°C)	233	233
Temperature difference between window's surfaces, ΔT	44.9	113.2
Maximum window temperature (°C)	490.67	584.36
Maximum window thermal stress (MPa)	51.12	128.77

thickness is reduced by 1 mm in the centre of the window. Figure 14 is a schematic view of the window thickness with the improved design.

Thickness of the window directly affects the window surface temperature (figures 15 and 16). Therefore, maximum window surface temperature of the improved design (window thickness is 2 mm) decreases by 93.36°C which is below the design limit (table 8). Thermal stress of the window also decreases by 77.65 MPa, which is lower than the window's elastic limit (175 MPa).

5. Conclusion

Thermal-hydraulic analysis of the window part of the spallation target is very important because the highest temperature is in the window part, where the stagnation point occurs, which explains why the window is not properly cooled. At the same time, the temperature

difference between the window's outer surface and the inner surface produces the thermal stress. If the thermal stress exceeds the design limit of the window wall, it could damage the window material. So, the thermal stress on the window is another important point, which should be taken into account in the target design.

The simulation results show that turbulence intensity, inlet temperature, mass flow rate of LBE flow and window thickness are sensitive to window surface temperature. Finally, best cooling of the window was obtained when the thickness of the window is 2 mm.

References

[1] John D Anderson Jr, *Computational fluid dynamics* (McGraw-Hill Inc., New York, 1995)
[2] F Sordo, P T Leon and J M Martinez-Val, *Nucl. Instrum. Methods in Phys. Res.* **A574**, 232 (2007)
[3] N Tak, H Neitzel and X Cheng, *Nucl. Engng. Design* **235**, 761 (2005)
[4] V Sobolev (SCK,CEN, Belgium) and G Benamati (ENEA, Italy), *Handbook on lead–bismuth eutectic alloy and lead*, http://www.oecd-nea.org/science/reports/2007/pdf/chapter2.pdf
[5] Thermo-physical properties of Pb–Bi and Pb, http://www.iaea.org/NuclearPower/Downloads/SMR/CRPI25001/2006/ANL%20Pb%20Data%201.pdf
[6] M Ashrafi-Nik and K Samec, *Thermo-hydraulic optimization of EURISOL-DS target* PSI report TM-34-06-0 (2006)
[7] A Abanades, F Sordo, A Lafuente and J M Martinez-Val, *Energy Conversion and Management* **49**, 1934 (2008)
[8] F Sordo, A Abanades, A Lafuente, J M Martinez-Val and M Perlado, *Nucl. Engng. Design* **239**, 2573 (2009)